Melting and Solidification of TiNi Alloys by Cold Crucible Levitation Method, and Evaluation of their Characteristics

Kazuhiro Matsugi[1], Hiroshi Mamiya[1], Yong-Bum Choi[1],
Gen Sasaki[1], Osamu Yanagisawa[1] and Hideaki Kuramoto[2]

[1]Department of Mechanical Materials Engineering,

Hiroshima University, Higashi-Hiroshima, 739-8527, Japan

[2] Hiroshima City Industrial Promotion Center,

Hiroshima, 7300052, Japan

e-mail address:

Kazuhiro Matsugi: matsugi@hiroshima-u.ac.jp

Hiroshi Mamiya: jazz-child@hotmail.co.jp

Yong-Bum Choi: ybchoi@hiroshima-u.ac.jp

Gen Sasaki: gen@hiroshima-u.ac.jp

Osamu Yanagisawa: yanagi@mec.hiroshima-u.ac.jp

Hideaki Kuramoto: hide22@itc.city.hiroshima.jp

ABSTRACT
The addition of Re, Fe and Cr into Ti-50mol%Ni has been carried out to improve the oxidation and mechanical properties. The mono phase consisting of TiNi with the B2 type structure was identified in micro-alloyed materials proposed on the basis of the d-electrons concept. Experimentally TiNi alloys were melted and solidified by the cold crucible levitation method (CCLM). The TiNi-(Cr, Fe, Re) alloys with high purity and without contamination from a crucible were prepared, and the homogeneous microstructure was achieved by the diffusion mixing effect of CCLM even in the as-cast alloys which contained Re and Cr with higher melting temperatures and different specific gravities. All alloys were caused the transformation from austenite to martensite phases below or above room temperature. The some alloys had the ability of shape memory even at room temperature. Ternary alloys showed higher flow stress level compared with the binary TiNi alloy. On the other hand, the oxidation at 1273K was promoted by the formation of titanium oxides (TiO_2) on the alloy surfaces. The oxidation resistance was improved by the formation of the continuously Cr_2O_3 film in TiNi-Cr alloys. The alloying effects by ternary elements (Re, Fe, Cr) in the intermetallic TiNi as well as metallic materials were explained well using two parameters used in the d-electrons concept.

Keywords: shape memory alloys, levitation melting, electron theory, oxidation resistance, ternary TiNi, alloy design, high purity, environmentally friendly materials;

1. Introduction

Among various shape memory alloys, TiNi alloys are the most commercially exploited ones because of their superior shape memory effect and super-elasticity, better mechanical properties, higher corrosion resistance and excellent biocompatibility[1-3]. These properties depend greatly on the exact chemical composition, processing history and smallness of undesirably dissolved elements[4]. Contaminants such as oxygen and carbon can dramatically affect the properties of TiNi alloys. Their penetration occurs basically during production and processing of alloys[5].

Commercial production process usually involves induction melting of alloys under heavy vacuum. A major source of contaminants is refractory melting crucibles, which needs to be carefully chosen. Numerous investigators [6-8] have tried to solve above problems, but they have generally not been able to obtain a satisfying result, because the contaminating behavior of ordinary materials (oxides, borides, silisides, sulfides, nitrides, fluorides, Mo_3Al and W) could never be totally stopped. It has been reported that Y_2O_3 stabilized with 8 to 15 wt% of Ti has the excellent performance in suppression for reaction between molten TiNi and crucibles, although these crucibles are very expensive[9]. In contrast, interaction between ZrO_2-, Al_2O_3- or SiC-crucibles and molten TiNi was investigated and discussed in the point of thermodynamic calculation[5]. Moreover, utilization of crucibles made of CaO is useful for melting Ti and its alloys, because of their refining effects

such as de-oxidation, de-sulfurization and de- nitrification[10]. CaO crucibles are very expensive and the handling is difficult due to their hydration.

Vacuum induction and arc skull melting processes both are used to prevent the molten metal contamination. These processes possessed, however, very low energy efficiency and great difficulty in obtaining sufficient superheats generally needed for a better molten metal homogenization[11]. The vacuum induction melting technique using the graphite crucibles for melting of TiNi, has been developed wherein the carbon contamination of the melt can be reduced significantly by adopting certain materials arrangement scheme[12].

Ti and Ni are difficult to be combined uniformly in composition as a solid alloy using usual furnaces like arc or induction melting furnaces, because molten Ti or TiNi is very chemically reactive at high temperature. To resolve these problems, utilization of the cold crucible levitation melting (CCLM) is very useful. CCLM in a high frequency induction furnace has both upper and lower electric coils which were utilized for heating and levitation of molten metals as a major function, respectively [13-15]. The molten metal is levitated by the eddy current in melting crucible which is water cooled. The alloys can be melted under untouched condition between melt and melting crucible, which leads to no contaminant from melting crucible. Moreover, TiNi alloys with uniform composition can be produced independently from the

difference in specific gravity or melting point between Ti and Ni, by the diffusion mixing effect of strong stirring due to an electromagnetic force.

The addition of Re, Fe or Cr to Ti-50mol%Ni has been carried out to improve the oxidation and mechanical properties. The kinds and amount of micro-alloying elements were determined on the basis of the d-electrons concept[16] which had been applied to design of high performance alloys, such as Ni, Ti and Fe-based alloys, etc[17-19]. The purpose of this paper is to determine oxidation and mechanical properties of TiNi-(Cr, Fe, Re) produced by the CCLM technique.

2. Experimental procedures

2.1 Alloy design

Two calculated parameters are mainly utilized in the d-electrons concept[16,17]. The one is the d-orbital energy level (Md) of alloying transition elements, and the other is the bond order (Bo) that is a measure of the covalent bond strength between atoms. The values of the parameters for each element which were calculated on octahedral cluster model (M_2X_4, M:alloying elements, X:Ti, using as MTi compounds), are listed in Table 1[20].

The Md parameter is associated with the phase stability of alloys[17] because the phase boundaries could be indicated by Md[16]. On the other hand, Bo parameter may be related in some way to the strength of alloys[17,21]. As micro-alloying elements of Cr, Re or Fe

and their amount were chosen showing higher Bo and similar Md values, compared with a TiNi of B2-type compound, in order to keep the high strength and B2 structure, respectively. Md and Bo values of TiNi are -1.284 and 0.466, respectively. Moreover, some oxides consisting of Cr or Re show excellent oxidation resistance at high temperatures[22]. The nominal compositions of experimental alloys proposed in this study are listed in Table 2, appending their Bo and Md which are simply obtained by taking the compositional average of the Bo and Mo values[20]. The binary TiNi and ternary TiNi-0.5Re alloys listed in Table 2 were produced as chemical compositions of Ti-49.7mol%Ni (hereafter called TiNi, Alloy compositions are referred to in mole per cent, unless otherwise noted.) and Ti-49.1Ni-0.5Re (hereafter called TiNi-0.5Re), respectively.

2.2 Experiments

All ingots were prepared from raw materials of Ni, Ti, Cr, Re or Fe with purity of 99.3, 99.7, 99.9, 99.96 or 99.9%, respectively, by CCLM under the atmosphere of argon gas with purity of 99.99%. The principle of levitation melting is illustrated in Fig.1. Each element was inserted in the copper melting crucible with 150cm^3 consisting of 24 segments. The alloys can be melted under untouched condition between melt and melting crucible, which leads to no contaminant from the melting crucible.

Figure 2 shows profiles of temperature in molten metal,

electric power in upper and lower coils and pressure in atmosphere of a furnace- chamber. The temperature was directly measured by insertion of thermocouples in molten metals. Molten metals with 120cm^3 were poured into the cold mold with an inner diameter of 13mm and length of 100mm, via the hole of melting crucible after levitation melting of approximately 330s. All ingots were heat-treated at 1273K for 173ks in an argon stream and water-quenched. Transformation behavior was investigated by differential scanning calorimetry (DSC) in the temperature range from 193 to 373K at rate of 5K/min in a nitrogen stream. Specimens for tensile tests were heat-treated at 723K for 3.6ks in an argon stream and water-quenched, for the occurrence of shape memory ability. Tensile tests were conducted on selected specimens with gauge diameters of 5mm and gauge lengths of 20mm, at room temperature under an initial strain rate of 5.0 x 10^{-4} s^{-1} in air. Oxidation tests at 1273K were carried out by a thermo-gravimetric method which meant measurements of weight gain of the specimens exposed in air for 72ks. Size of the oxidation specimen was 3 x 3 x 4mm. Rockwell hardness number on C scale was measured at room temperature. X-ray diffraction (XRD) analysis employing nickel filtered Cu-K_α radiation was performed for phase identification.

3. Results and Discussion

3.1 Microstructures and effects of CCLM

Some XRD patterns of alloys are shown in Fig.3. All

experimental alloys had B_2 or B_2 and $B_{19'}$ types structures depending on M_s-temperatures which were shown below or above room temperature, respectively. The XRD pattern of the as-cast TiNi-5Cr is compared with that of the heat treated one, as seen in Fig.3(d) and (e). Same XRD patterns were observed between both conditions, which meant the better homogenization of molten metal by the diffusion mixing effect of CCLM even for addition of Re or Cr with higher melting temperatures and densities, compared with other techniques such as induction and arc skull meltings[11].

Contents of impurities such as oxygen, carbon and nitrogen in the TiNi prepared by the CCLM, were 0.046, 0.009 and 0.004wt%, respectively. The contents of gaseous impurities of oxygen and nitrogen were lower than those (oxygen and nitrogen: 0.069 and 0.006 wt%, respectively) in the raw materials, because of highly vacuum level as shown in Fig.2. In contrast, there was the same value (0.009 wt%) of the carbon content between the TiNi alloy and raw material. This content of carbon in TiNi is lower than that (0.07wt%) in TiNi alloys prepared by vacuum induction melting in the graphite crucible[12]. Moreover, it is found from the contents of impurities that the cleanly molten metals were created by utilization of CCLM without the reaction between the molten metal and water-cooled copper crucible, although the affinity of Ti with oxygen, carbon and nitrogen was strong.

Figure 4 shows the DSC curves of TiNi, TiNi-1.5Fe and TiNi-5Cr alloys. Upper and lower lines represent the exothermic and

endothermic curves, respectively. In TiNi, the transformation on cooling and heating curves occurred in one step from austenite to martensite (A to M) and from martensite to austenite (M to A), respectively. In contrast, two-step transformations on heating and cooling curves were observed on Fe and Cr containing alloys. Two steps on heating correspond to the reverse transformations of martensite to R phase (M to R) and R phase to austenite (R to A). Moreover, two steps on cooling correspond to austenite to R phase (A to R) and R to M transformations. Whereas two transformations on cooling were well separated, two reverse transformations on heating overlapped, making it impossible to measure the finish of the M to R transformation and the start of the R to A transformation. In TiNi-1.5Fe, the cooling transformation was similar to that of TiNi-1Cr, but with the R to M appearing as a broader peak.

3.2 Mechanical properties

It is suggested from results of XRD and DSC that TiNi and TiNi-Re, -Fe, and -Cr are mainly in austenite state at room temperature. Figure 5 shows the true stress-strain curves obtained from TiNi, TiNi-0.5Re and TiNi-1.0, -5Cr. Specimens of TiNi and TiNi-0.5Re were strained up to 4% and then the applied stress was released. Strains of approximately 3.5 and 3.1% remained after releasing the applied stress in TiNi and TiNi-0.5Re, respectively. Moreover, the rest deformation was recovered with heating above A_f

(austenite finish) temperature. Remained strains of 0.1 and 0.8% were observed even after heating above A_f temperature on TiNi and TiNi-0.5Re, respectively.

TiNi showed the finally fracture-stress and -elongation of approximately 1000MPa and 15%, respectively, and their values were near to those obtained from the vacuum-induction melted TiNi[12]. Ternary alloys with Cr or Re showed higher flow stress than binary TiNi, although two tensile tests of TiNi-Cr were interrupted before completely plastic deformation because of solidification-defect with approximately 200μm size in specimens. This defect was caused as the cold shut due to the turbulent flow of molten metals in the pouring.

3.3 Oxidation properties

Kinetic oxidation curves at 1273K are shown in Fig.6. The accelerated oxidation curves of TiNi and TiNi-0.5Re shows the complicated shape showing several plateaus. The oxidation was severe initially, settled down for a while, and then was catastrophic again. The severe and moderate oxidation took place alternately, which meant formation of porous TiO_2 and TiO oxides at the interface between alloys and air, and their exfoliation. This agrees with the previously open literature[23]. In contrast, the simply oxidation curves without a plateau were obtained on TiNi-Cr, which meant formation of densely Cr_2O_3 oxide. For TiNi-5Cr, the almost constant value was shown in the weight gain after 72ks, which was

caused due to the increase of continuously Cr_2O_3 oxide films. Moreover, TiNi-5Cr showed the excellent oxidation resistance and its weight gain after 72ks was approximately 30%, compared with TiNi.

The apparent activation energy for the initial oxidation of TiNi was estimated to 180 kJ/mol which was close to that (183 kJ/mol)[24] of oxidation in Ti-2.6Al. In contrast, the values in apparent activation energy for oxidation of TiNi-5Cr and pure Cr were estimated to 200kJ/mol in this study and reported to 245kJ/mol[25], respectively, which suggested the difference in oxidation behavior between Cr-addition and –nonadditon alloys. In other words, Cr_2O_3 oxide films are effective for the suppression of oxygen-diffusion toward TiNi-Cr alloys, because the activation energy of TiNi-5Cr was estimated as the value between those of TiNi and pure Cr. The rate in oxidation becomes to small, as the amount in formation of continuously Cr_2O_3 oxide films increases in Cr containing alloys.

3.4 Evaluation of alloying effects by Bo and Md parameters

All alloys had the B2 type structure, regardless of kinds and amount of ternary micro-alloying elements (Re, Fe, Cr). As shown in Fig.7, the ternary alloys in this study are located on the structure map which is constructed using Bo and Md for the 3d transition-metal based compound (MTi, M : binary alloying elements)[20,26]. Any intermetallic compound has more than two

sublattices in crystal. So, when a third element is added into the compound, it is first necessary to take into account the substitutional site of the element, and hence attention is directed toward this substitutional problem. It is found that the structure map of binary MTi can be also applied for ternary NiTi-Re, -Fe, and -Cr compounds with compositions proposed in this study, although above substitutional problem can not be clarified for ternary alloying elements.

The A_s (austenite start) temperatures measured by the DSC method correlated well with the Md and Bo parameters showing alloying effects, as seen in Figs.8, 9, respectively. This agrees with the previously report explaining the estimation of β transus by Md and Bo for many Ti alloys[27]. The γ' solvus temperatures were also evaluated by the Bo and Md diagram for superalloys[21]. In contrast, the amounts in formation of the δ ferrite at 1323K for ferritic steels and in crystallized eutectic γ' phase of superalloys were also estimated by Md[28,29]. In contrast, the A_f temperatures as well as A_s correlated well with the Md and Bo parameters. It is noted that the transition temperatures of intermetallic compounds are also predicted accurately by Md and Bo.

There was a good correlation between the hardness data and Bo. As Bo increased in alloys, the hardness increased monotonously, as shown in Fig.10. Morinaga reported the relation between Bo and the change in hardness with the alloying additions to Ni_3Al[30]. Solid solution hardening of Ni_3Al may be affected by electric or

chemical factors[31] in addition to the lattice strain factor (i.e. atomic size factor). The correlation shown in Fig.10 agrees with that obtained from Ni_3Al.

There was a good correlation between the weight gain by oxidation after 72ks and Bo. As Bo increased in alloys, the weight gain decreased linearly, as shown in Fig.11, although there were a few data. It has been found that various physical properties could be interpreted in term of Bo. For example, Bo correlated well with activation energies for atomic diffusion[32]. The active oxidation may be interpreted by Bo. The result shown in Fig.11 indicates that an increase in the bond strength between atoms leads to high oxidation resistance. This agrees with the result obtained from the active corrosion rate of Ti alloys in 10%H_2SO_4 at 343K[33].

It is found that the alloying effects by ternary elements (Re, Fe, Cr) on the mechanical, oxidation and physical properties were explained well using two parameters (Bo, Md) used in the d-electrons concept even for intermetallic compounds, as well as metallic materials such as Ni, Ti, Al, Mg and Fe-based alloys, etc[17-19,34].

4. Conclusions

(1) The homogeneous microstructure was achieved by the diffusion mixing effect of CCLM even in the as-cast alloys which contained Re and Cr with higher melting temperatures and different specific gravities, compared with alloys prepared by

other techniques such as induction and arc skull melting methods.

(2) The cleanly molten metals with lower contents of O, C, and N, were created by utilization of CCLM without the reaction between the molten metal and water-cooled copper crucible, although the affinity of Ti with oxygen, carbon and nitrogen was strong, which led fabrication of highly purity TiNi.

(3) The mono phase consisting of TiNi with the B2 type structure was identified in all micro-alloyed materials proposed on the basis of the d-electrons concept.

(4) All alloys showed the transformation from austenite to martensite phases below or above room temperature. The some alloys had the ability of shape memory even at room temperature. Ternary alloys showed higher flow stress level compared with the binary TiNi alloy.

(5) Oxidation at 1273K was promoted by the formation of the titanium oxide (TiO_2) on the alloy surfaces. The oxidation resistance was improved by the continuously formation of the Cr_2O_3 films in Cr added TiNi alloys.

(6) The alloying effects by ternary elements (Re, Fe, Cr) in the intermetallic TiNi as well as metallic materials, were explained well by two parameters (Bo, Md) used in the d-electrons concept.

References

1 K. Otsuka and X. Ren : *Intermetallics,*1999, **7**, 511-528.

2 J. Van Humbeek: *Mater. Sci. Eng.*, 1999, A273- A275,134-148.
3 T. Durieg, A. Pelton and D. Stockel: *Mater. Sci. Eng.*, 1999, **A273-A275**, 149-160.
4 'Material Properties Handbook, Titanium Handbook' (ed. T. W. During), 1994, ASM, Metal Park, OH, ASM.
5 S. K. Sadrnezhaad and S. B. Raz: *Metall. Trans. B*, 2005, **36B**, 395-403.
6 C. Berthod, C. Weber, W. M. Thompson, H. O. Bielstein and M. A.Schwartz:*J. Am. Ceram. Soc.*, 1975, **40**, 363-373.
7 M. Garfinkle and H. M. Davis:*Trans. ASM*, 1965, **58**, 520-530.
8 D. R. Schuyler and J. A. Petrusha : 'Casting of Low Melting Titanium Alloys, Vacuum Metallurgy',475-503; 1977, Princeton, NJ, Science Press.
9 R. L. Saha, T. K. Nandy, R. D. K. Misra and K. T. Jacob : *Metall. Trans. B,* 1990, **21B**, 559-66.
10 T. Degawa:*Bulletin of Japan Institute of Metals*, 1988, **27**, 466-473.
11 J. P. Kuang, R. A. Harding and J. Campbell: *Mater. Sci. Technol.*, 2000, **16**,1007-1016.
12 N. Nayan, Govind, C. N. Saikrishna, K. V. Ramaiah, S. K. Bhaumik, K. S. Nair and M. C. Mittal:*Mater. Sci. Eng.*, 2007, **A465**, 44-48.
13 H. Tadano, T. Take, M. Fujita and S. Hayashi: Proc. 2nd Int. Conf. 'Electromagnetic Processing of Materials', **1**, 1997, 377-382.
14 T. Volkmann, W. Loser and D.M. Herlach: *Metall. Trans. A*, 1997, **28A** , 461-469.
15 S. Asai:*J. Iron and Steel Institute of Japan*, 2002, **7**, 44-48.
16 M. Morinaga, N. Yukawa, H. Adachi and H. Ezaki :Proc. 5th Int. Conf. 'Superalloys', (ed. M.Gell e tal.), Warrendale, PA, October 1984, The Metallurgical Society of AIME, 523-532.
17 K. Matsugi, Y. Murata, M. Morinaga and N. Yukawa: *Mater.Sci.Eng.*,1993, **A172**, 101-110.
18 M.Morinaga, J.Saito and M.Morishita:*J. Japan Institute of Light Metals*, 1992, **42**, 614- 621.
19 M. Morinaga, Y. Murata and H. Ezaki: Proc. Int. Symp. 'Material Chemistry in Nuclear Environment',Tsukuba,

March 1992, 241-252

20 Y. Harada, M. Morinaga, J. Saito and Y. Takagi: *J. Phys. Condens. Matter*, 1997, **9**, 8011-8030.

21 K. Matsugi, Y. Murata, M. Morinaga and N. Yukawa: Proc. 7th Int. Conf. on 'Superalloys 1992', Pennsylvania, USA, September 1992, Minerals, Metals &Materials Society, 307-316.

22 K. Matsugi, M. Kawakami, Y. Murata, M. Morinaga, N. Yukawa and T. Takayanagi: *J. Iron and Steel Institute of Japan*, 1992, **78**, 821- 828.

23 C. L. Chu, S. K. Wu and Y. C. Yen: *Mater. Sci. Eng.* 1996, **A216**, 193-200.

24 A. M. Chaz, C. Coddet, and G. Beranger: *J. Less-Common Met.*, 1982, **83**, 49-70.

25 D. Caplan and G. I. Sproule: *Oxid. Met.* 1975, **9**, 459-472.

26 J. Saito, Y. Takagi, M. Morinaga, Y. Murata and Y. Harada: Proc. 3rd Japan Int. SAMPE Symp., Tokyo, December 1993, 1252-1257.

27 M. Morinaga, N. Yukawa, T. Maya, K. Sone and H. Adachi : Proc. 6th World Conf. on 'Titanium', Cannes, France, June 1988, 1601-1606.

28 M. Morinaga, R. Hashizume and Y. Murata : Proc. 5th Int. Conf. on 'Materials for Advanced Power Engineering', Liege, Belgium, October 1994, 319-328.

29 K. Matsugi, R. Yokoyama, Y. Murata, M. Morinaga and N.Yukawa : Proc. 4th Int. Conf. on 'High Temperature Materials for Power Engineering', Liege, Belgium, October 1990, 1251-1260.

30 M. Morinaga, N. Yukawa and Y. Murata : *J. Phys. Soc. Jpn.*, 1984, **53**, 653- 663.

31 R. W. Guard and J. H. Westbrook : *Trans. Met. Soc. AIME*, 1959, **215**(1959) 807.

32 M. Morinaga, N. Yukawa and H. Adachi :*J. Iron and Steel Institute of Japan*, 1985, **71**, 1441-1451.

33 M. Morishita, Y. Ashida, M. Chikuda, M. Morinaga, N. Yukawa and H. Adachi : *ISIJ Int.*, 1991, **31**, 890-896.

34 R. Ninomiya, H. Yukawa and M.Morinaga:*J. Japan Institute*

of Light Metals, 1994, **44**, 171- 177.

Table 1 Bo and Md values for elements.

Elements		Bo(d-3d)/Md	Elements		Bo(d-3d)/Md
3d	Ti	0.809/1.476	4d	Te	1.339/-0.062
	Cr	1.189/0.385		Ru	1.079/-0.612
	Mn	1.113/0.115		Rh	0.834/-1.473
	Fe	0.969/-0.293	5d	Hf	1.051/2.034
	Co	0.698/-0.679		Ta	1.291/1.589
	Ni	0.466/-1.284		Re	1.430/0.116
	Cu	0.138/-2.399		Os	1.158/-0.563
4d	Nb	1.240/1.325	Others	Al	0.358/1.105
	Mo	1.351/0.470		Si	0.334/-0.278

Table 2 Nominal compositions of experimental alloys proposed in this study.

Alloys	Bo/Md
Ti-50.0mol%Ni	0.466/-1.284
Ti-49.5mol%Ni-0.5mol%Re	0.476/-1.270
Ti-48.5mol%Ni-1.5mol%Fe	0.481/-1.254
Ti-49.0mol%Ni-1.0mol%Cr	0.480/-1.251
Ti-45.0mol%Ni-5.0mol%Cr	0.538/-1.117

List of figure captions

Fig.1 Schematic illustrations of principle of CCLM and cold die for pouring of melts.

Fig.2 Profiles of (a) temperature in molten metal, (b) electric power in two coils, and (c)pressure in atmosphere during CCLM process.

Fig.3 XRD profiles obtained from as-cast (a)TiNi, (b)TiNi-0.5Re, (c)TiNi-1.5Fe and (d)TiNi-5Cr, and (e) homogenized TiNi-5Cr.

Fig.4 DSC curves obtained from (a)TiNi, (b)TiNi-1.5Fe and (c)TiNi-1Cr.

Fig.5 True stress-strain curve of each alloy.

Fig.6 Kinetic oxidation curves obtained from exposure experiments for 72ks at 1273K for some experimental alloys.

Fig.7 The Bo-Md structure map[20,26] for the MTi compounds. Crystal structures are denoted using the Structurbericht symbol and also the Pearson's symbol.

Fig.8 Estimation for the A_s temperatures by Md.

Fig.9 Estimation for the A_s temperatures by Bo.

Fig.10 Change of Rockwell hardness number on C scale of experimental alloys with Bo.

Fig.11 Relation between the ratio of weight gain by oxidation after 72ks to initial weight and the Bo parameter.

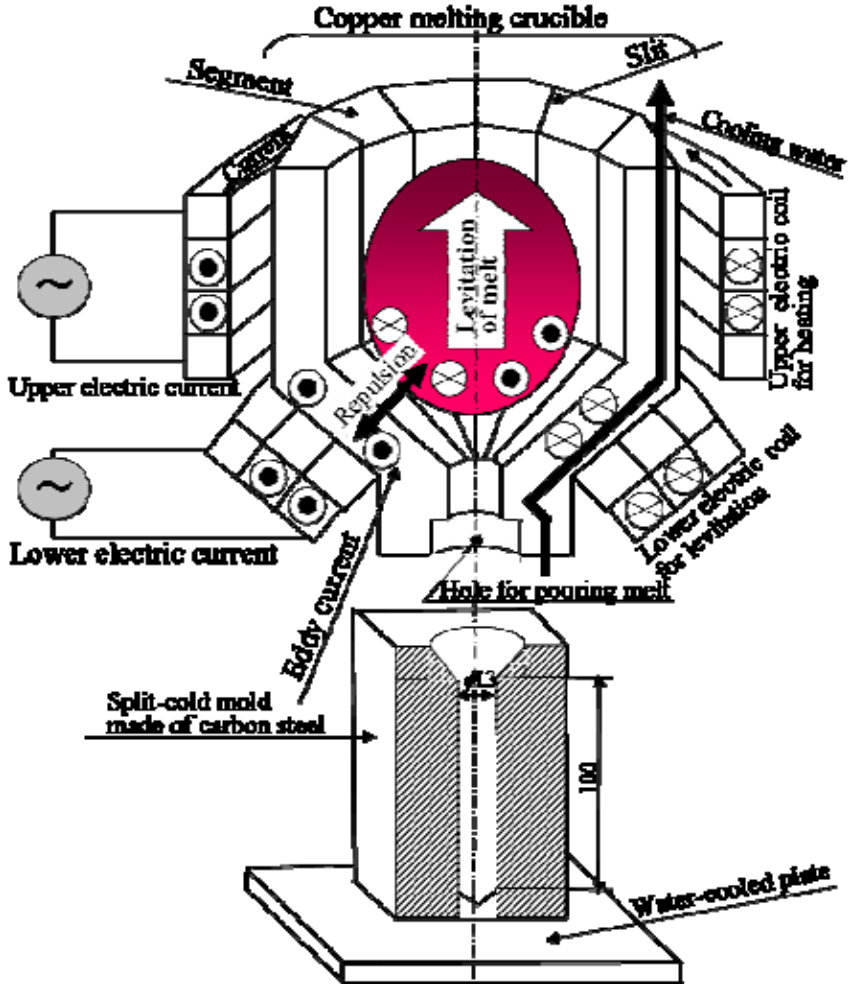

Fig.1 Schematic illustrations of principle of CCLM and cold die for pouring of melts.

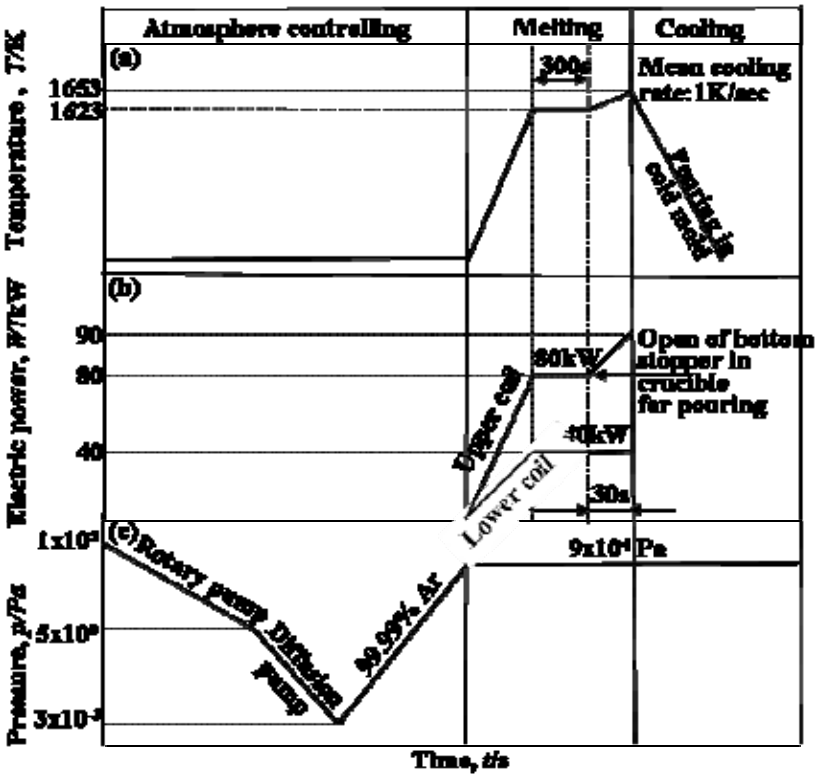

Fig.2 Profiles of (a) temperature in molten metal, (b) electric power in two coils, and (c)pressure in atmosphere during CCLM process.

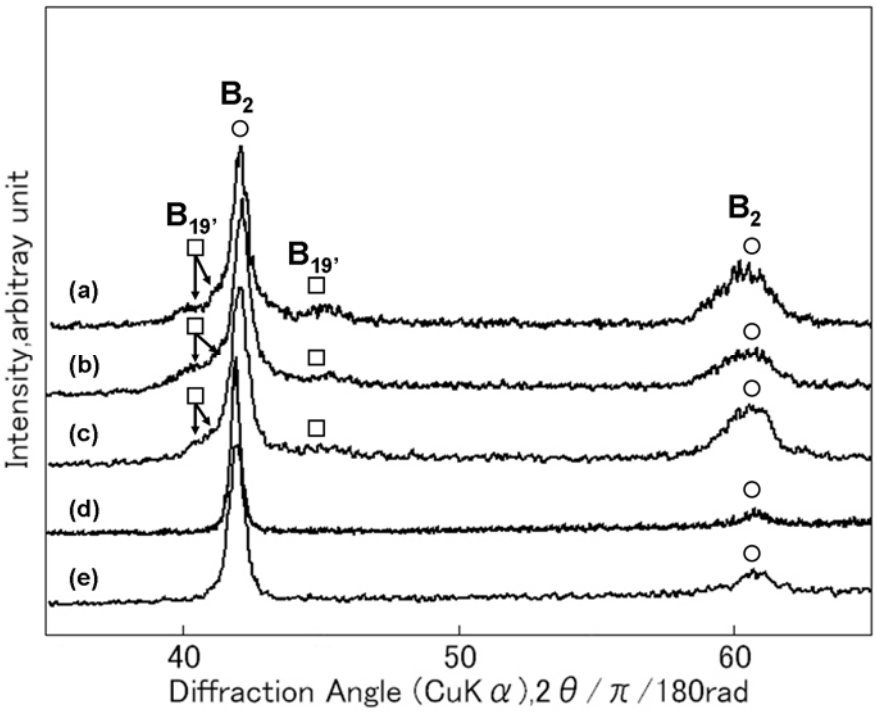

Fig.3 XRD profiles obtained from as-cast (a)TiNi, (b)TiNi-0.5Re, (c)TiNi-1.5Fe and (d)TiNi-5Cr, and (e) homogenized TiNi-5Cr.

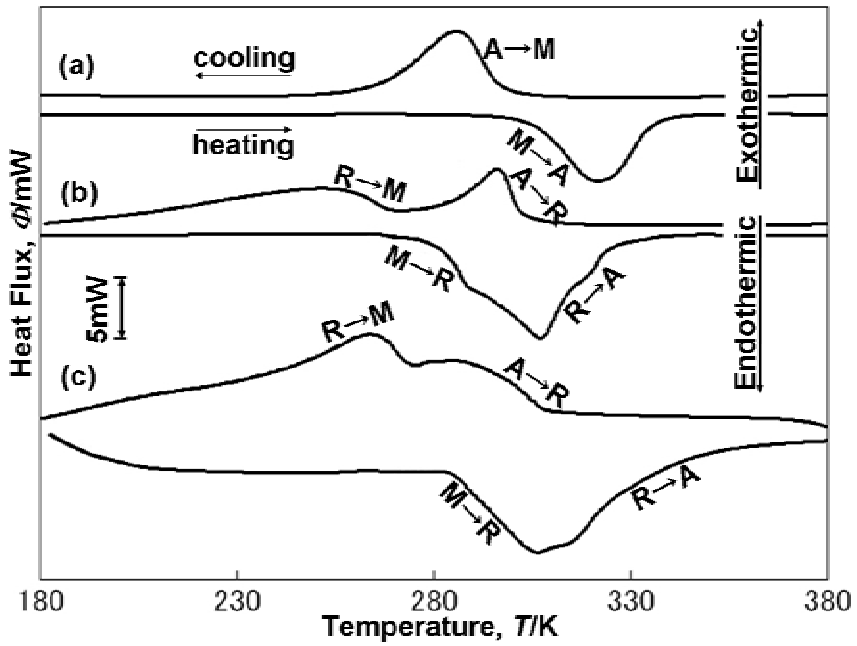

Fig.4 DSC curves obtained from (a)TiNi, (b)TiNi-1.5Fe and (c)TiNi-1Cr.

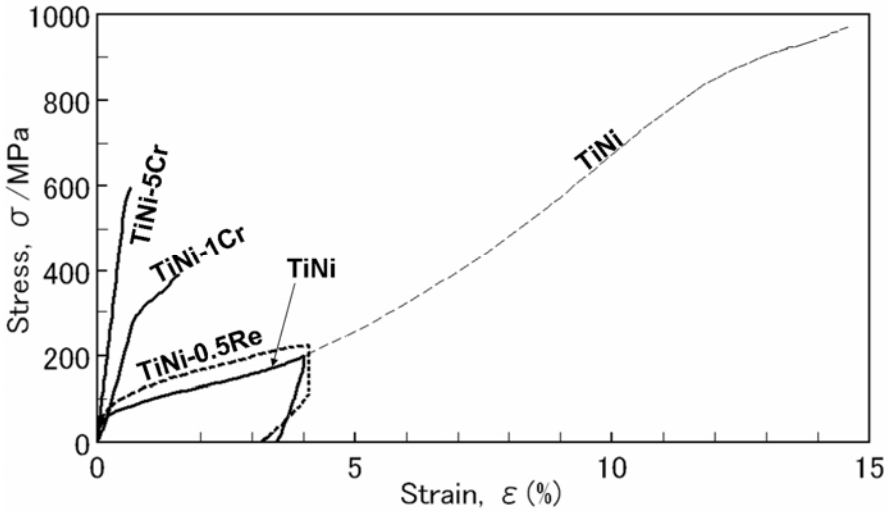

Fig.5 True stress-strain curve of each alloy.

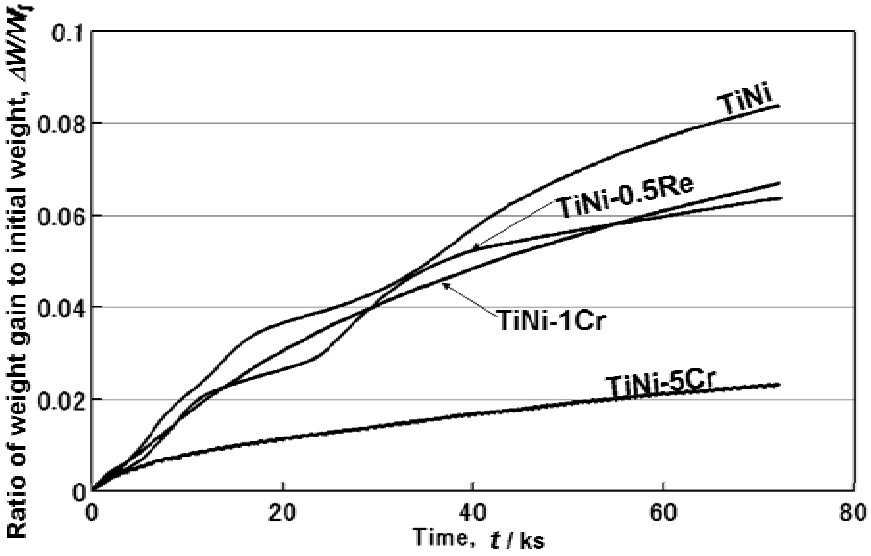

Fig.6 Kinetic oxidation curves obtained from exposure experiments for 72ks at 1273K for some experimental alloys.

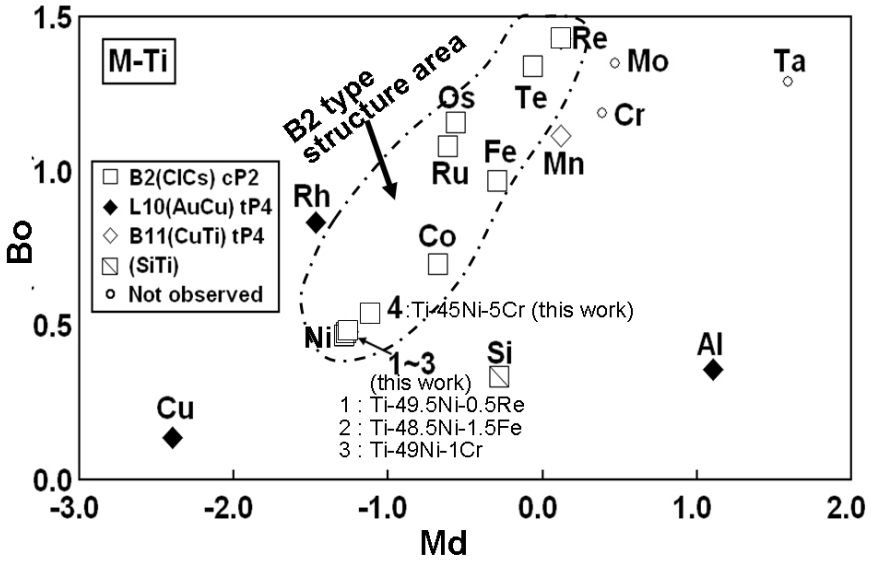

Fig.7 The Bo-Md structure map[20,26] for the MTi compounds. Crystal structures are denoted using the Structurbericht symbol and also the Pearson's symbol.

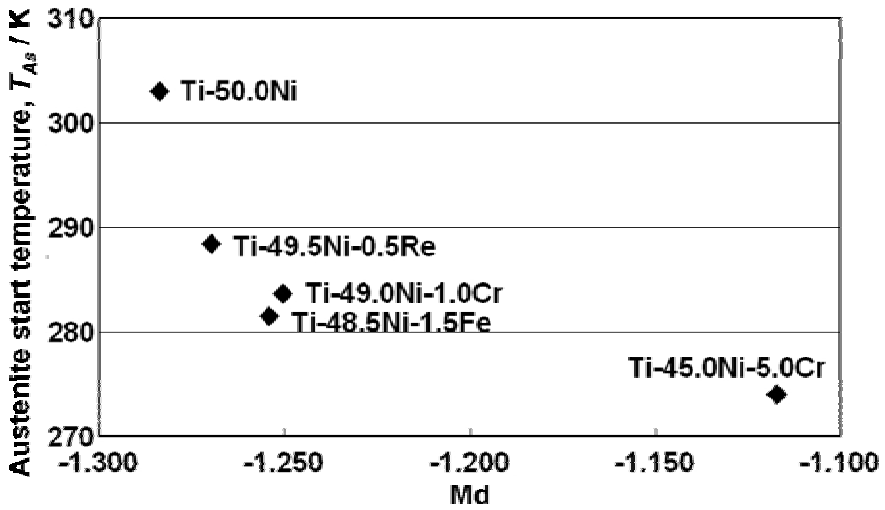

Fig.8 Estimation for the A_s temperatures by Md.

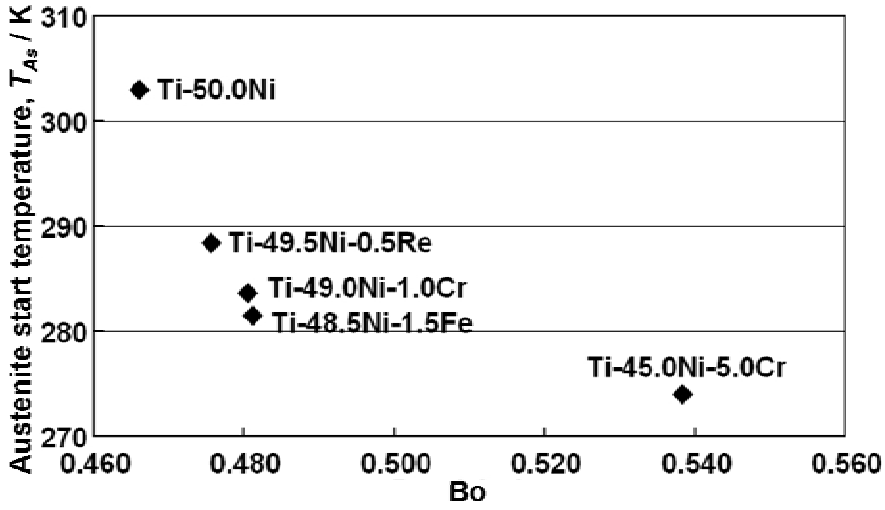

Fig.9 Estimation for the A_s temperatures by Bo.

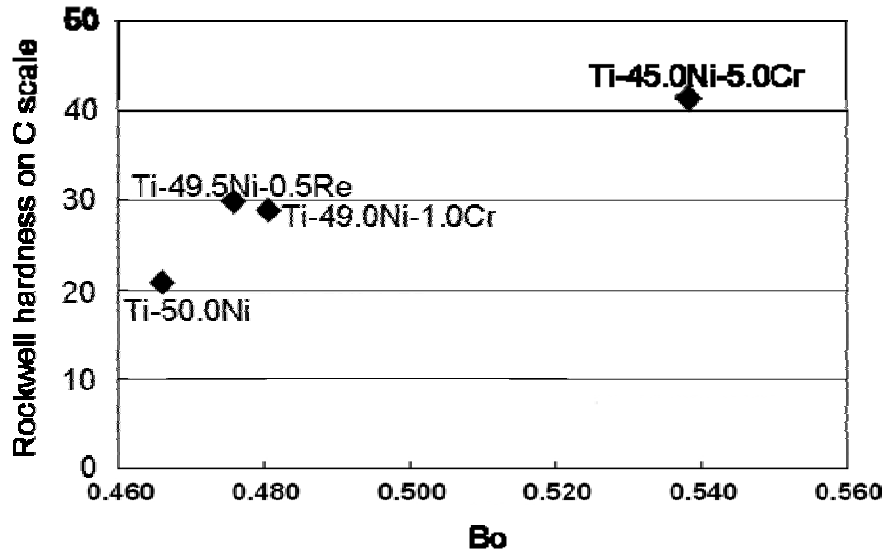

Fig.10 Change of Rockwell hardness number on C scale of experimental alloys with Bo.

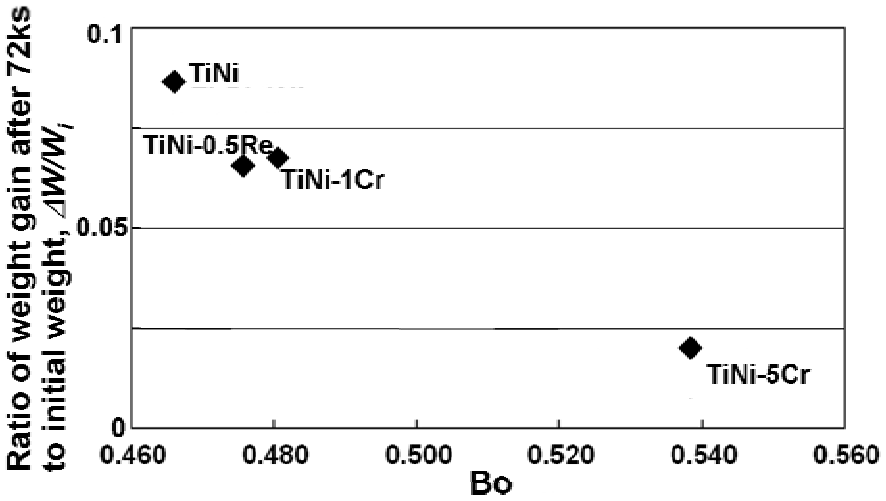

Fig.11 Relation between the ratio of weight gain by oxidation after 72ks to initial weight and the Bo parameter.